Geol. Mag. **156** (*5*), *2019, pp. 874–888* © *Cambridge University Press 2018*
doi:10.1017/S0016756818000250

Petrogenesis of plagiogranites in the Muslim Bagh Ophiolite, Pakistan: implications for the generation of Archaean continental crust

DANIEL COX*‡†, ANDREW C. KERR‡, ALAN R. HASTIE* & M. ISHAQ KAKAR§

*School of Geography, Earth and Environmental Sciences, University of Birmingham, Edgbaston, Birmingham, B15 2TT, UK
‡School of Earth and Ocean Sciences, Cardiff University, Main Building, Park Place, Cardiff, CF10 3AT, UK
§Centre of Excellence in Mineralogy, University of Balochistan, Quetta, Pakistan

(*Received* 3 August 2017; *accepted* 27 February 2018; *first published online* 2 April 2018)

Abstract – High-SiO_2 rocks referred to as oceanic plagiogranites are common within the crustal sequences of ophiolites; however, their mode of petrogenesis is controversial with both late-stage fractional crystallization and partial melting models being proposed. Here, we present new whole-rock data from plagiogranitic dyke-like bodies and lenses from the lower and middle sections of the sheeted dyke complex of the Cretaceous Muslim Bagh Ophiolite, northwestern Pakistan. The plagiogranites have similar geochemical signatures that are inconsistent with them being the fractionation products of the mafic units of the Muslim Bagh Ophiolite. However, the plagiogranites all display very low TiO_2 contents (<0.4 wt %), implying that they formed by partial melting of mafic rocks. Melt modelling of a crustal gabbro from the Muslim Bagh Ophiolite shows that the trace-element signature of the plagiogranites can be replicated by 5–10 % melting of a crustal hornblende gabbro with amphibole as a residual phase, resulting in a concave-up middle rare Earth element pattern. Compositional similarities between the Muslim Bagh Ophiolite plagiogranites and Archaean TTG (trondhjemite–tonalite–granodiorite) has implications for the generation of juvenile Archaean continental crust. As the Muslim Bagh Ophiolite was derived in a supra-subduction zone, it is suggested that some Archaean TTG may have been derived from melting of mafic upper crust in early subduction-like settings. However, due to the small volume of Muslim Bagh Ophiolite plagiogranites, it is inferred that they can be instructive on the petrogenesis of some, but not all, Archaean TTG.

Keywords: Pakistan, Muslim Bagh, ophiolite, oceanic plagiogranite, partial melting

1. Introduction

Within obducted Phanerozoic ophiolite sequences, suites of felsic rocks termed 'oceanic plagiogranites' (Coleman & Peterman, 1975; Le Maitre *et al*. 2002, p. 118) occur as small-volume (<10 %) components (Coleman & Peterman, 1975; Koepke *et al*. 2007). The petrogenesis of these plagiogranites is controversial, having been variously proposed to have formed by the late-stage crystallization of mafic melts (Coleman & Peterman, 1975), hydrous partial melting (and assimilation) of mafic rocks (Gerlach, Leeman & Ave Lallemant, 1981; Amri, Benoit & Ceuleneer, 1996; Gillis & Coogan, 2002; France, Ildefonse & Koepke, 2009; France *et al.* 2010; Erdmann *et al*. 2015) or silicate–liquid immiscibility (Dixon & Rutherford, 1979).

Significantly, plagiogranites have compositional similarities to trondhjemite, tonalite and granodiorite (TTG) rocks that are common in Archaean terranes from the period 4.0–2.5 Ga (e.g. Drummond, Defant & Kepezhinskas, 1996; Kerrich & Polat, 2006; Moyen & Martin, 2012; Kusky *et al*. 2013). Although themselves controversial, Archaean TTG are considered, by many, to be generated by the partial melting of mafic igneous source regions (e.g. Drummond, Defant & Kepezhinskas, 1996; Foley, Tiepolo & Vannucci, 2002; Rapp, Shimizu & Norman, 2003; Martin *et al*. 2005; Moyen & Stevens, 2006; Nutman *et al*. 2009; Hastie *et al*. 2015, 2016). Significantly, the compositional similarity of Phanerozoic oceanic plagiogranites to Archaean TTG suggests that, if we can better understand how plagiogranites are formed, it may further our understanding of how primitive continents were formed on the early Earth (Rollinson, 2008, 2009, 2014).

In this paper, we present major- and trace-element data for oceanic plagiogranites sampled from a sheeted dyke complex within the Late Cretaceous (Neo-Tethyan) Muslim Bagh Ophiolite in northwestern Pakistan (Kakar *et al*. 2012). We investigate the composition of these plagiogranitic lenses and dykes in the sheeted dyke complex to determine their petrogenesis. We then discuss the implications of these results for the generation of Archaean continental crust.

2. Ophiolites and plagiogranites

Oceanic plagiogranites are found throughout geological time, in strata of both Precambrian (e.g. Samson *et al*. 2004; Kaur & Mehta, 2005) and

†Author for correspondence: DXC506@student.bham.ac.uk

Phanerozoic (e.g. Tilton, Hopson & Wright, 1981; Flagler & Spray, 1991; Rollinson, 2009) age, and are common in the crustal sections of ophiolitic sequences (e.g. Flagler & Spray, 1991; Amri, Benoit & Ceuleneer, 1996; Twining, 1996; Yaliniz, Floyd & Goncuoglu, 2000; Samson *et al*. 2004). Plagiogranites have also been recovered from recent oceanic ridge systems around the world, for example the Southwest Indian (e.g. Dick *et al*. 2000), Central Indian (e.g. Nakamura *et al*. 2007) and Mid-Atlantic ridges (e.g. Aranovich *et al*. 2010; Grimes *et al*. 2011). The morphology of oceanic plagiogranites is complex and they have been documented in a range of intrusive forms from small veins (millimetre- to centimetre-scale; e.g. Dick *et al*. 2000; Nakamura *et al*. 2007), to dykes and inclusions (millimetre- to metre-scale; e.g. Flagler & Spray, 1991; Jafri, Charan & Govil, 1995), to large kilometre-scale plutonic bodies (e.g. Rollinson, 2009).

Oceanic plagiogranites are predominantly composed of sodic plagioclase and quartz, with mafic (usually hornblende and pyroxene) minerals being minor constituents (<10 %) and K-feldspar being a rare phase. In addition to the major modal mineralogy, several accessory minerals including zircon, magnetite and ilmenite are also commonly found in oceanic plagiogranites (Coleman & Peterman, 1975; Coleman & Donato, 1979).

In the mid-1970s, plagiogranites were considered to represent the likely silicic end-products of crystallizing basaltic magmas (Coleman & Peterman, 1975; Coleman & Donato, 1979). Although such a crystallization model is still advocated by some authors, who have shown that oceanic plagiogranites fall along the liquid lines of descent of evolving magmas in other ophiolite units (e.g. Jafri, Charan & Govil, 1995; Rao, Rai & Kumar, 2004; Freund *et al*. 2014), the genesis of oceanic plagiogranites is more commonly attributed to the partial melting of mafic igneous source regions (Gerlach, Leeman & Ave Lallemant, 1981; Flagler & Spray, 1991; see Koepke *et al*. 2007 for a review of oceanic plagiogranite petrogenesis models). Melting models propose that oceanic plagiogranites are derived through partial melting of mafic protoliths, either by hydrous partial melting of crustal gabbros (e.g. Gerlach, Leeman & Ave Lallemant, 1981; Flagler & Spray, 1991; Amri, Benoit & Ceuleneer, 1996) or the assimilation and partial melting of hydrothermally altered sheeted dykes (e.g. Gillis & Coogan, 2002; France, Ildefonse & Koepke, 2009; France *et al.* 2010; Erdmann *et al*. 2015).

A partial melting origin is supported by the experimental work of Koepke *et al*. (2004), who undertook hydrous melting experiments on oceanic cumulate gabbros at temperatures from 900 – 1060 °C and a relatively shallow pressure of 0.2 GPa. Koepke *et al*. (2004) showed that lower temperature runs (900 – 940 °C) generated partial melts with similar major element compositions to natural oceanic plagiogranites. One important finding from the P-T experiments was that the melts replicate the low TiO_2 concentrations that can be found in oceanic plagiogranites (<1 wt %; Koepke *et al*. 2004). Low TiO_2 is now considered a key characteristic of oceanic plagiogranites that have been derived by partial melting, as opposed to oceanic plagiogranites derived through fractional crystallization that display higher TiO_2 contents (>1 wt %; Koepke *et al*. 2004, 2007). Further experimental work conducted by France *et al*. (2010) has also shown that oceanic plagiogranites derived by partial melting have low TiO_2 contents, supporting the experimental work of Koepke *et al*. (2004).

3. Geological setting

3.a. Regional setting

The Muslim Bagh Ophiolite (MBO) is one of a number of ophiolites (i.e. Bela, Waziristan, Khost, Zhob) of Neo-Tethyan origin (Kakar *et al*. 2014) that comprise the Western Ophiolite Belt of the Zhob Valley, northwestern Pakistan (Ahmad & Abbas, 1979; Mahmood *et al*. 1995; Gnos, Immenhauser & Peters, 1997) (Fig. 1). These ophiolites represent fragments of Neo-Tethyan Ocean crust that were obducted onto the margin of the Indian continent prior to its final collision with Asia (e.g. Gnos, Immenhauser & Peters, 1997; Khan *et al*. 2009); they therefore mark the boundary between the Indian and Eurasian plates (Asrarullah, Ahmad & Abbas, 1979; Mengal *et al*. 1994; Gnos, Immenhauser & Peters, 1997).

The Muslim Bagh area comprises four main geological units (Fig. 1). These units are (south to north) the Indian Passive Margin, the Bagh Complex, the MBO and the Flysch Belt (Mengal *et al*. 1994; Kakar *et al*. 2014). Triassic–Paleocene sediments of the Indian Passive Margin (Kakar *et al*. 2014) are overthrust by the Mesozoic Bagh Complex along the Gawal Bagh thrust (Mengal *et al*. 1994). The Bagh Complex comprises a series of thrust-bounded units including a melange unit, two volcanic units (basalt-chert unit (Bbc), hyaloclastite-mudstone unit (Bhm)) and a sedimentary unit (Bs); see Mengal *et al*. (1994) for detailed descriptions of each unit. Thrusted over the Bagh Complex is the MBO (Kakar *et al*. 2014), described in more detail in the following section. The uppermost unit is the Eocene–Holocene Flysch Belt that rests unconformably on top of the MBO and Bagh Complex in the Katawaz Basin (Mengal *et al*. 1994; Qayyum, Niem & Lawrence, 1996; Kasi *et al*. 2012). The Flysch Belt can be broadly divided into four thrust-bounded formations (Nisai, Khujak, Multana and Bostan formations) comprising fluvial and deltaic successions (Qayyum, Niem & Lawrence, 1996; Kasi *et al*. 2012).

3.b. Muslim Bagh Ophiolite

The MBO is exposed as two massifs: the Saplai Tor Ghar and Jang Tor Ghar massifs (Ahmad & Abbas, 1979; Mahmood *et al*. 1995; Gnos, Immenhauser &

https://doi.org/10.1017/S0016756818000250 Published online by Cambridge University Press

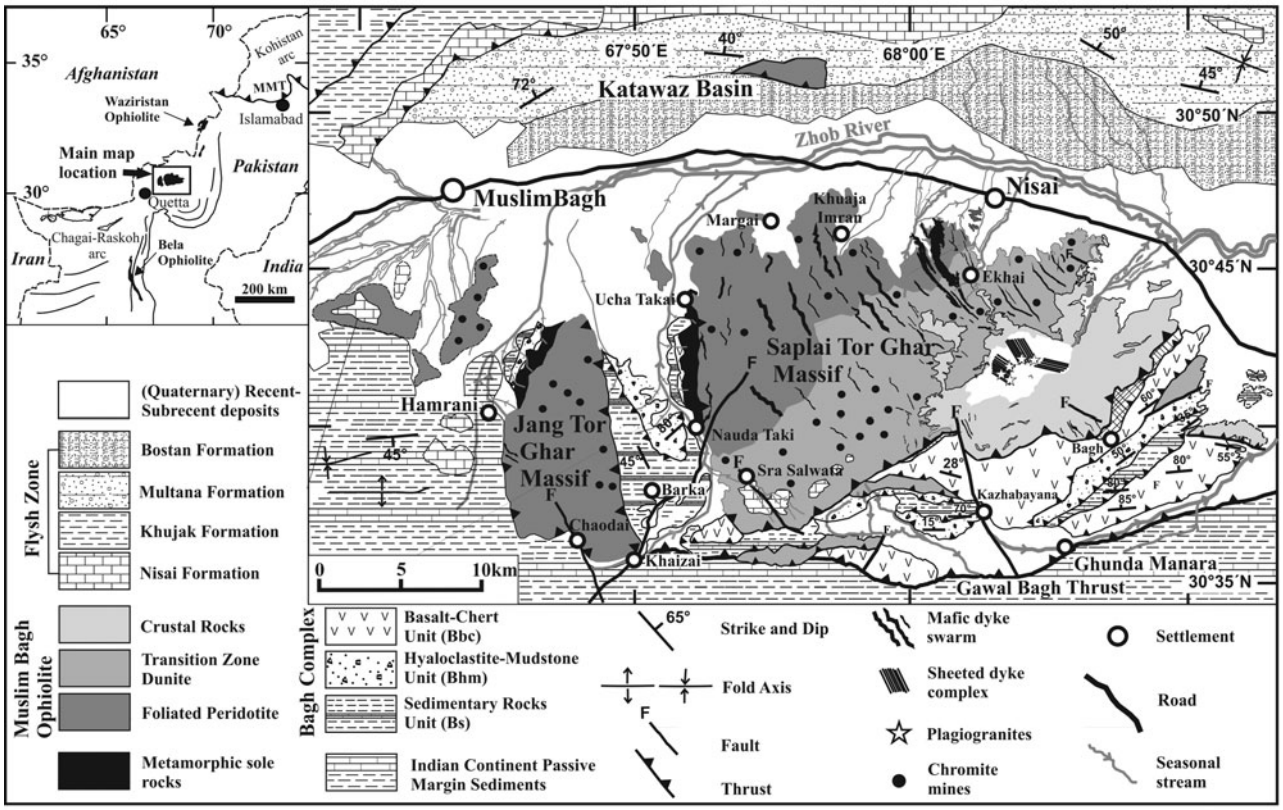

Figure 1. Geological map of the Muslim Bagh area. Inset highlights the location of the Muslim Bagh Ophiolite in northwestern Pakistan (modified from Kakar *et al*. 2014).

Peters, 1997) (Fig. 1). The tectonic setting of formation of the MBO has been variously interpreted as a mid-ocean ridge (Mahmood *et al*. 1995), a back-arc basin (Siddiqui *et al*. 1996) or an island arc (Khan, Kerr & Mahmood, 2007). Most recently however, Kakar *et al*. (2014) have presented evidence that the MBO formed above a slow-spreading supra-subduction zone, based on both the structure of the ophiolite and its arc-like geochemistry. Recent U–Pb dating of zircons in MBO plagiogranites by Kakar *et al*. (2012) gave a crystallization age of 80.2 ± 1.5 Ma, similar to the *c.* 82–81 Ma K–Ar ages obtained by Sawada *et al*. (1995). Dating of amphiboles from the sub-ophiolitic metamorphic sole have yielded K–Ar and plateau Ar/Ar ages of 80.5 ± 5.3 Ma (Sawada *et al*. 1995) and 70.7 ± 5 Ma (Mahmood *et al*. 1995), respectively. The younger age of 70.7 ± 5 Ma (Mahmood *et al*. 1995) is interpreted to date the age of emplacement of the MBO which, when taken in conjunction with the crystallization age of the ophiolite, suggests that the ophiolite was obducted soon after formation (e.g. Kakar *et al*. 2014).

The Saplai Tor Ghar Massif displays a near-complete ophiolite sequence (Kakar *et al*. 2014), with only the extrusive basalts absent (Mahmood *et al*. 1995). The Jang Tor Ghar Massif only preserves mantle sequence rocks (i.e. foliated peridotite) of the oceanic lithosphere, however (Mahmood *et al*. 1995; Kakar *et al*. 2014). The mantle sequence of the MBO has been divided into a foliated peridotite section and mantle–crust transition zone (Kakar *et al*. 2014). The foliated peridotite is located in both massifs, and comprises serpentinized harzburgite with minor dunite and chromite deposits (Mahmood *et al*. 1995; Khan, Kerr & Mahmood, 2007; Kakar *et al*. 2014). Lherzolite is also found in the lower part of the mantle sequence (Kakar *et al*. 2014). The mantle–crust transition zone of the MBO is a dunite-rich zone with minor gabbro, wherlite, pyroxenite and chromite only exposed in the Saplai Tor Ghar Massif (Mahmood *et al*. 1995; Khan, Kerr & Mahmood, 2007; Khan, Mahmood & Casey, 2007; Kakar *et al*. 2014). Chromite bodies of the transition zone are larger than those in the foliated peridotite section of the mantle sequence (Kakar *et al*. 2014).

The oceanic crustal sequence, as exposed in the Saplai Tor Ghar Massif, comprises a 200–1500 m thick ultramafic–mafic cumulate zone (Ahmad & Abbas, 1979; Siddiqui *et al*. 1996) and a 1 km thick, poorly developed sheeted dyke complex (Siddiqui *et al*. 1996; Khan, Kerr & Mahmood, 2007). The ultramafic–mafic cumulate zone displays both single and cyclic sequences grading from basal dunite through pyroxenite to gabbro, with infrequent anorthosite at the top of the cumulate zone (Ahmad & Abbas, 1979; Siddiqui *et al*. 1996; Khan, Kerr & Mahmood, 2007; Kakar *et al*. 2014). Above the cumulate zone, the sheeted dykes are doleritic, dioritic and plagiogranitic in composition, and all display greenschist to amphibolite grade metamorphism (Sawada *et al*. 1995; Kakar *et al*. 2014).

https://doi.org/10.1017/S0016756818000250 Published online by Cambridge University Press

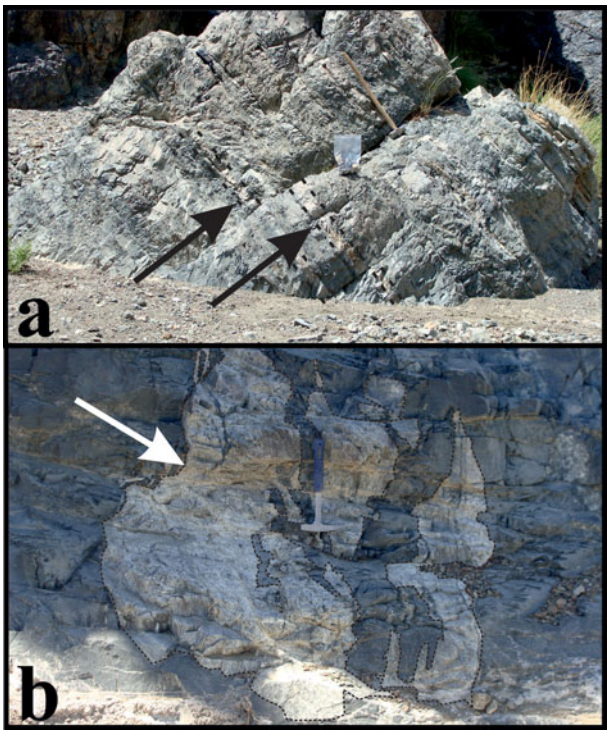

Figure 2. (Colour online) Field photographs of the Muslim Bagh Ophiolite plagiogranites. Plagiogranites are exclusively located within the sheeted dyke complex of the ophiolite crustal sequence, where they take the form of (a) dyke-like bodies and (b) lenses.

Plagiogranites of the MBO are exclusively located at the base and middle portions of the sheeted dyke complex (Mahmood *et al*. 1995; Siddiqui *et al*. 1996). The plagiogranites are rare, comprising <5 % by volume of the sheeted dyke complex, and take the form of dykes and small lenses (Fig. 2). They are discontinuous, intrusive bodies, sometimes tapering, displaying a range of sizes. Lenses range from 0.1×0.3 to 1.0×3.0 m, with more dyke-like bodies ranging from 0.3×1.0 to 1.5×3.0 m. The plagiogranites have sharp contacts with the enclosing sheeted dykes, and have also undergone greenschist-amphibolite facies metamorphism with foliated to mylonitized textures (Sawada *et al*. 1995; Siddiqui *et al*. 1996; Kakar *et al*. 2014). Samples for the current study were collected from a range of separate plagiogranite dykes and lenses from across the region. The general sampling locality is shown on Figure 1; more detailed localities and sample information are given in Supplementary Table S1 (available at http://journals.cambridge.org/geo).

4. Petrography

The plagiogranites sampled from the MBO for the current study are predominately composed of quartz (*c*. 40 vol. %) and plagioclase (*c*. 50 vol. %), with hornblende and pyroxene comprising minor amounts (<<10 vol. %; hornblende > pyroxene) and zircon and Fe-Ti oxides common as accessory phases. Phenocryst phases of plagioclase, quartz, hornblende and pyroxene are surrounded by a fine groundmass composed of plagioclase, quartz, hornblende, pyroxene, potassium feldspar (rare) and accessory phases. All phenocryst phases have subhedral to anhedral crystal shapes, with plagioclase displaying simple and albite twinning; hornblende twinning is rare. Throughout the sections, quartz is composed of sub-grains. However, unlike Coleman & Peterman's (1975) original definition of oceanic plagiogranites, the MBO plagiogranites do not display vermicular intergrowths of quartz and plagioclase. Evidence for hydrothermal alteration and low-grade metamorphism includes moderate sericitization of plagioclase crystals (concentrated in the core of crystals; see online Supplementary Figure S1, available at http://journals.cambridge.org/geo).

5. Geochemical results

5.a. Analytical techniques

Plagiogranite samples were prepared and analysed for major, minor and trace elements at the School of Earth and Ocean Sciences, Cardiff University, Wales, UK. Loss on ignition (LOI) was measured using *c*. 1.5 ± 0.0001 g of sample powder baked at 900 °C in a Vecstar Furnace for 2 hours. Major and minor elements and Sc were measured using a JY-Horiba Ultima 2 inductively coupled plasma optical emission spectrometry (ICP-OES). Minor, trace and the rare Earth elements (REE) were measured using a thermoelemental X series (X7) inductively coupled plasma mass spectrometer (ICP-MS) following methods described by McDonald & Viljoen (2006). The accuracy and precision of the data were assessed using the international standard reference materials JB1a, JA2 and JG-3 (obtained analysis, certified values and detection limits for JB1a are shown in Supplementary Table S2, available at http://journals.cambridge.org/geo). The full plagiogranite sample dataset is shown in Table 1.

5.b. Element mobility

The altered nature of the plagiogranite samples means that some of the major elements and large-ion lithophile elements (LILE) may have been mobilized relative to the high-field-strength elements (HFSE) and REE (e.g. Hastie *et al*. 2007). Although low LOI values (0.59–2.45 wt %) suggest that the plagiogranites have suffered little alteration, the high proportion of quartz (*c*. 40 %) means that the effective LOI of the non-quartz components may double the whole-rock values. However, major element (v. LOI) variation plots of the plagiogranite samples show no correlation with LOI, all displaying very low R^2 values (see Supplementary Fig. S2, available at http://journals.cambridge.org/geo). With the exception of MgO (<0.52), all major elements display R^2 values of <0.32. These data suggest that the major-element concentrations are not primarily controlled by alteration, and can confidently be used to compare with literature Archaean TTG

https://doi.org/10.1017/S0016756818000250 Published online by Cambridge University Press

Table 1. Major- and trace-element analyses of the Muslim Bagh Ophiolite plagiogranites.

Sample	Pl-01	Pl-02	Pl-03	Pl-06	Pl-07	Pl-13	Pl-15	Pl-17	Pl-19	Pl-21	Pl-22	Pl-23	Pl-25
SiO_2 (wt %)	73.08	70.71	70.26	70.00	71.66	72.06	72.40	74.06	74.85	74.69	72.56	79.73	76.85
TiO_2	0.30	0.31	0.30	0.34	0.30	0.31	0.34	0.30	0.29	0.29	0.39	0.10	0.28
Al_2O_3	12.98	14.83	14.87	15.50	15.63	15.03	13.37	10.50	13.42	13.79	14.41	12.27	11.68
$Fe_2O_{3(T)}$	2.81	3.48	3.00	2.47	2.40	2.60	2.84	4.03	3.02	2.79	4.47	1.25	3.87
MnO	0.04	0.05	0.04	0.04	0.04	0.04	0.04	0.03	0.03	0.02	0.04	0.01	0.04
MgO	1.81	1.01	0.78	0.66	0.63	0.42	0.92	1.22	0.50	0.40	0.37	0.10	0.19
CaO	3.68	2.87	3.02	3.94	3.38	4.01	5.67	4.72	4.01	3.93	3.10	1.91	1.86
Na_2O	3.12	4.42	4.35	4.19	4.34	4.24	3.13	1.70	3.40	3.65	3.98	4.20	4.14
K_2O	0.52	0.98	0.64	0.62	0.71	0.55	0.43	0.33	0.18	0.17	0.29	1.06	0.12
P_2O_5	0.03	0.03	0.04	0.05	0.05	0.05	0.06	0.06	0.07	0.07	0.14	0.02	0.06
LOI	1.83	1.71	1.75	1.16	1.32	0.81	1.09	2.45	0.82	0.76	1.72	0.59	0.81
Total	100.19	100.38	99.05	98.97	100.46	100.12	100.29	99.40	100.05	99.99	100.92	100.53	99.22
Sc (ppm)	6.7	7.8	9.0	10.7	11.8	12.5	13.4	13.0	13.4	9.4	7.3	2.9	10.5
V	59	64	55	45	38	55	45	48	62	44	49	10	8
Cr	13	26	2	13	8	7	80	174	12	21	116	18	10
Co	8.6	14.8	13.5	7.9	5.6	7.1	9.3	13.7	6.8	7.3	6.6	2.0	14.3
Ni	15.7	50.2	22.4	78.5	10.4	8.9	8.6	10.5	25.3	5.0	89.1	10.1	14.2
Ga	10.9	11.3	10.7	11.0	10.4	11.2	11.2	8.8	11.6	12.1	15.8	10.0	12.1
Rb	3.8	6.1	3.4	2.4	2.9	2.8	4.1	8.1	2.0	1.5	2.9	20.7	1.6
Sr	160	163	167	170	144	163	159	196	155	155	214	105	91
Y	13.0	13.6	11.3	17.3	18.0	14.2	15.8	17.7	19.4	16.3	13.0	17.9	22.0
Zr	40.3	198.8	46.6	94.9	42.7	51.2	20.7	35.2	80.0	57.8	283.0	61.1	129.8
Nb	1.28	1.05	1.17	0.79	0.69	0.68	0.80	0.80	0.89	1.42	4.13	5.19	0.70
Cs	0.05	0.07	0.10	0.07	0.09	0.06	0.05	0.12	0.04	0.03	0.07	0.13	0.02
Ba	68	69	71	79	74	71	78	67	60	80	198	502	59
La	5.14	2.87	2.97	3.70	2.12	3.28	2.14	3.16	1.50	1.69	21.83	15.45	4.77
Ce	9.58	6.28	6.08	7.89	5.06	6.47	5.00	6.50	4.26	4.56	37.17	27.28	11.27
Pr	1.15	0.84	0.84	1.09	0.77	0.84	0.75	0.94	0.70	0.71	4.23	3.03	1.70
Nd	4.68	3.71	3.91	5.22	3.99	3.89	3.72	4.52	3.51	3.43	14.97	10.13	7.69
Sm	1.37	1.28	1.21	1.59	1.44	1.35	1.50	1.50	1.43	1.33	2.96	2.15	2.31
Eu	0.53	0.53	0.63	0.68	0.60	0.58	0.63	0.65	0.52	0.54	0.82	0.54	0.88
Gd	1.54	1.38	1.33	1.96	1.96	1.69	1.78	1.91	2.00	1.73	2.86	2.27	2.76
Tb	0.28	0.27	0.24	0.38	0.35	0.30	0.33	0.35	0.42	0.35	0.40	0.37	0.51
Dy	1.88	1.88	1.71	2.53	2.67	2.01	2.35	2.45	2.90	2.34	2.12	2.30	3.09
Ho	0.43	0.45	0.38	0.56	0.60	0.46	0.51	0.53	0.60	0.49	0.40	0.50	0.64
Er	1.41	1.38	1.10	1.74	1.81	1.42	1.61	1.68	1.85	1.46	1.18	1.57	1.84
Tm	0.24	0.26	0.19	0.30	0.31	0.24	0.28	0.27	0.31	0.27	0.19	0.30	0.33
Yb	1.58	1.75	1.22	2.04	2.03	1.46	1.76	1.80	2.07	1.68	1.24	2.15	2.13
Lu	0.24	0.30	0.19	0.32	0.32	0.22	0.26	0.27	0.31	0.27	0.21	0.34	0.33
Hf	1.42	5.81	1.48	2.90	1.37	1.65	0.72	1.15	2.08	1.57	6.72	1.43	3.04
Ta	0.11	0.07	0.14	0.10	0.06	0.06	0.07	0.07	0.06	0.10	0.29	0.47	0.04
Pb	1.34	1.39	2.48	1.88	1.41	1.80	1.27	1.17	1.11	0.64	1.82	3.45	1.62
Th	2.17	0.51	0.25	0.26	0.20	0.20	0.23	0.47	0.45	0.33	11.92	4.95	0.61
U	0.30	0.10	0.11	0.09	0.07	0.06	0.05	0.12	0.09	0.09	0.93	0.95	0.13

$Fe_2O_{3(T)}$: total iron

data. Additionally, Sr (v. LOI; Supplementary Fig. S3, available at http://journals.cambridge.org/geo) also displays a very low R^2 value of <0.45. Consequently, the following discussion focuses on the major elements and HFSE and REE, generally regarded as relatively immobile up to greenschist facies (e.g. Floyd & Winchester, 1975; Pearce & Peate, 1995; Hastie *et al.* 2007, 2009).

5.c. Major elements

The plagiogranites display a relatively narrow, high-SiO_2 range (70.8–80.2 wt %, anhydrous values), with most also having relatively high Al_2O_3 (10.7–15.8 wt %) and Na_2O (1.7–4.5 wt %) contents (Fig. 3). Samples have low TiO_2 (<0.4 wt %), MgO (0.1–1.8 wt %) and K_2O (<1.1 wt %). Al_2O_3, MnO (not shown), MgO and K_2O decrease with increasing SiO_2, while other oxides such as TiO_2, Na_2O, $Fe_2O_{3(T)}$ and CaO show little to no correlation (Fig. 3). Further, the plagiogranites do not fall on clear liquid lines of descent along with the gabbros and sheeted dykes of the MBO. On a normative ternary An–Ab–Or plot, the plagiogranites classify as tonalites and trondhjemites (Fig. 4).

The major-element abundances of the plagiogranites are very similar to those of Archaean TTG (Condie, 2005; Martin *et al.* 2005; Moyen & Martin, 2012), with TTG compositions consistently plotting at the lower SiO_2 end of the plagiogranite compositions (Fig. 3). However, this similarity is not observed in K_2O contents, with TTG generally having much higher K_2O contents (1.65–2.22 wt %) compared with the MBO plagiogranites (<1.1 wt %).

5.d. Trace elements

The plagiogranites show no convincing intra-formation fractionation trends on trace-element variation plots (Fig. 5). This is not surprising, considering

https://doi.org/10.1017/S0016756818000250 Published online by Cambridge University Press

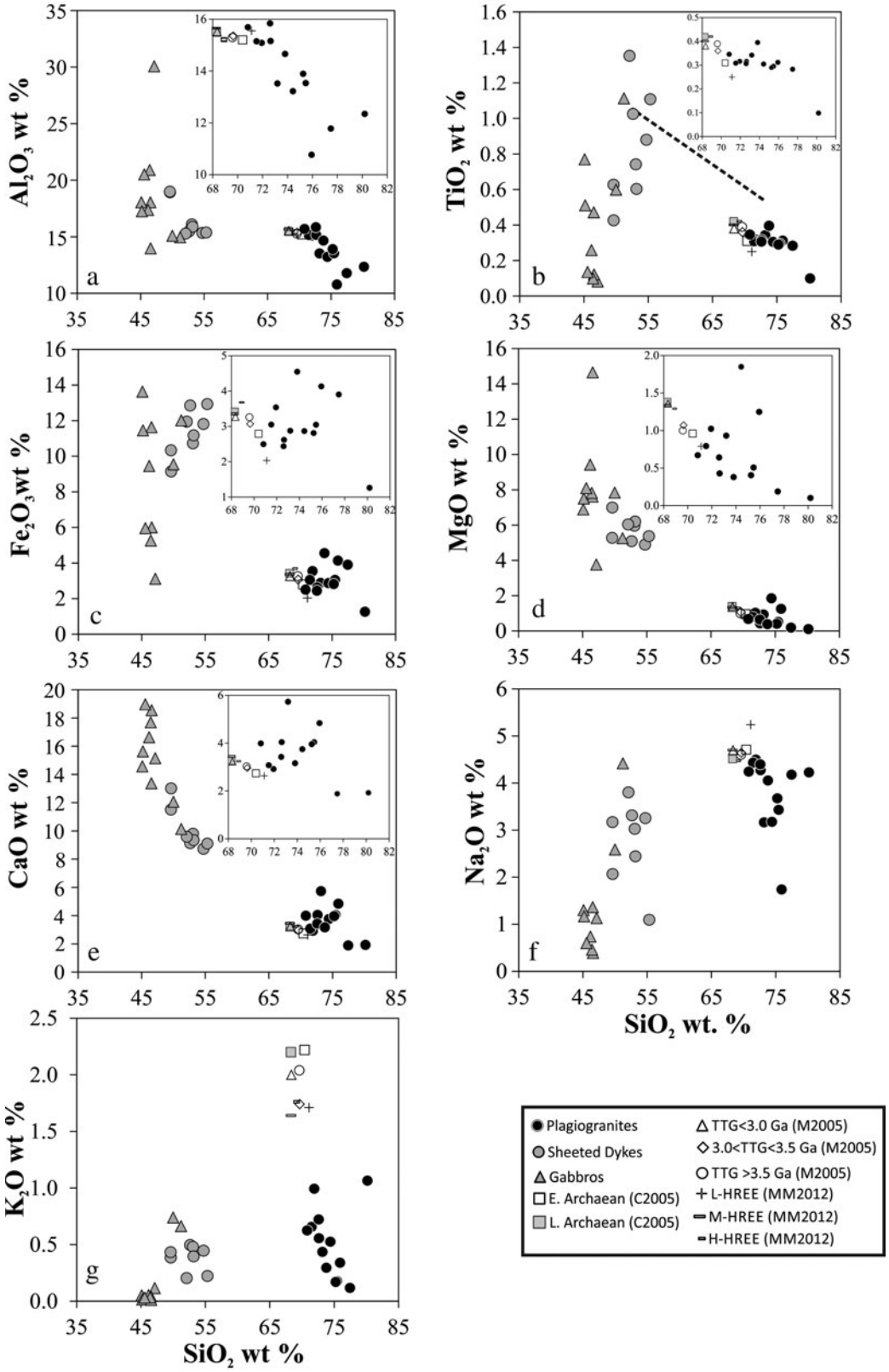

Figure 3. (a–g) Major-element variation plots (v. SiO_2) of the Muslim Bagh Ophiolite plagiogranites. Also plotted are the sheeted dykes and gabbros of the crustal section of the Muslim Bagh Ophiolite (data from Kakar *et al*. 2014) and Archaean TTG average compositions; C2005 (Condie, 2005), M2005 (Martin *et al*. 2005) and MM2012 (Moyen & Martin, 2012). The black dashed line in (b) separates plagiogranites derived by hydrous partial melting (below the line) and those plagiogranites derived through differentiation or liquid immiscibility (above the line) (after Koepke *et al*. 2007).

https://doi.org/10.1017/S0016756818000250 Published online by Cambridge University Press

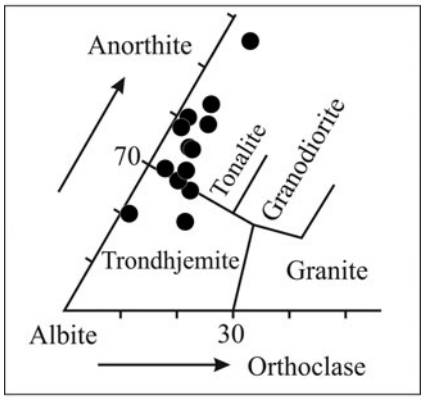

Figure 4. Normative An–Ab–Or ternary plot. Muslim Bagh Ophiolite plagiogranites classify as either tonalites or trondhjemites. Fields from Barker (1979).

that the samples are collected from a diverse range of geographically distinct dykes and lenses. The plagiogranites span a wide range in Zr concentrations (*c.* 20–280 ppm), although the majority of samples fall in the range 20–90 ppm; only three have higher concentrations (130, 199, 283 ppm), suggestive of zircon accumulation (e.g. Rollinson, 2009). In general, the plagiogranites have lower trace-element concentrations than the sheeted dyke complex of the MBO and, with the exception of Sr, have trace-element contents similar to, or slightly greater than, the majority of the gabbros of the crustal section of the ophiolite (Fig. 5). As is the case with the major elements (Fig. 3), the plagiogranites do not fall on clear liquid lines of descent along with the gabbros and sheeted dykes of the MBO (Fig. 5). As seen above, the major-element compositions of the MBO plagiogranites are very similar to those of TTG compositions (Fig. 3); however, this similarity is not as evident for the trace elements (Fig. 5).

The plagiogranites show broadly coherent trends in the middle- to heavy-REE (M/HREE) on chondrite-normalized REE plots, but have variable light-REE (LREE) contents, from markedly enriched to relatively depleted patterns (e.g. 4.8–0.7 $(La/Sm)_N$; Fig. 6a, c). The LREE-enriched patterns shown by the majority of the plagiogranite samples are inconsistent with the original definition of plagiogranites (Coleman & Peterman, 1975), and are shown to be enriched relative to the well-studied crustal plagiogranites from the Oman and Troodos Ophiolites (Fig. 6a). However, plagiogranites from the Sjenica (Milovanovic *et al.* 2012) and Tasriwine (Samson *et al.* 2004) ophiolites with LREE-enriched patterns have recently been reported (Fig. 6a). When compared with Archaean TTG compositions, plagiogranite samples are not as enriched in LREE (Fig. 6a). Most samples also show a slight chondrite-normalized enrichment in the heaviest REE relative to MREE, and display small U-shaped (concave upwards) patterns. The U-shaped patterns can be quantified using the Dy/Dy* ratio of Davidson, Turner & Plank (2012), which ranges over 0.96–0.43 (Fig. 6b). Most plagiogranites have weak positive Eu anomalies (1.06–1.51 (Eu/Eu)*), with only three samples having negative Eu anomalies (0.74–0.94; Fig. 6c). Interestingly, two of the three samples with negative Eu anomalies are also significantly enriched in LREE.

On normal mid-ocean-ridge basalt (N-MORB) normalized multi-element plots most plagiogranites display relatively flat patterns at concentrations just below N-MORB, with positive Th anomalies and negative Nb–Ta–Ti anomalies (Fig. 7a). Zr and Hf contents vary from enriched to depleted, relative to N-MORB. Most samples also have positive Sr anomalies; however, three samples have negative Sr anomalies, two of which display corresponding negative Eu anomalies (Fig. 6c).

6. Discussion

The modal abundance of quartz and plagioclase in combination with the low K_2O contents (<1.1 wt %) of the MBO plagiogranites is similar to oceanic plagiogranites found elsewhere (e.g. Gerlach, Leeman & Ave Lallemant, 1981; Amri, Benoit & Ceuleneer, 1996; Rollinson, 2009). Additionally, the trace-element compositions of plagiogranites from the Muslim Bagh, Oman and Troodos ophiolites all show a high degree of compositional overlap (Fig. 7a, plagiogranite field) (Rollinson, 2009; Freund *et al.* 2014). Nevertheless, the LREE-enriched and slightly concave-upwards MREE patterns of the majority of MBO samples are distinct relative to the original oceanic plagiogranite definition (Coleman & Peterman, 1975; Coleman & Donato, 1979).

High SiO_2 (>70 wt %) and Na_2O (3<Na_2O<4.5 wt %) concentrations and low modal K-feldspar contents, low K_2O/Na_2O ratios and low $Fe_2O_3 + MgO + MnO + TiO_2$ (most < 5 wt %) of the MBO plagiogranites make them compositionally similar to Archaean TTG as defined by Martin *et al.* (2005) and Moyen & Martin (2012). Additionally, when compared with Archaean TTG compositions on an N-MORB normalized multi-element plot, the plagiogranites display broadly similar concentrations, overlapping the TTG field at the lower LREE and higher HREE concentrations (Fig. 7b).

6.a. Plagiogranite petrogenesis

The majority of plagiogranites display enrichment in LREE relative to HREE (Fig. 6c), and all plagiogranites have negative Nb–Ta and positive Th anomalies (Fig. 7a). Additionally, the N-MORB-like concentrations of the other trace elements suggest that the plagiogranites (Fig. 6c) were generated at a MOR setting with a subduction input, likely a supra-subduction zone. This supports recent work by Kakar *et al.* (2014) who propose a supra-subduction model for the formation of the MBO. However, the petrogenesis of oceanic plagiogranites is controversial; fractional

https://doi.org/10.1017/S0016756818000250 Published online by Cambridge University Press

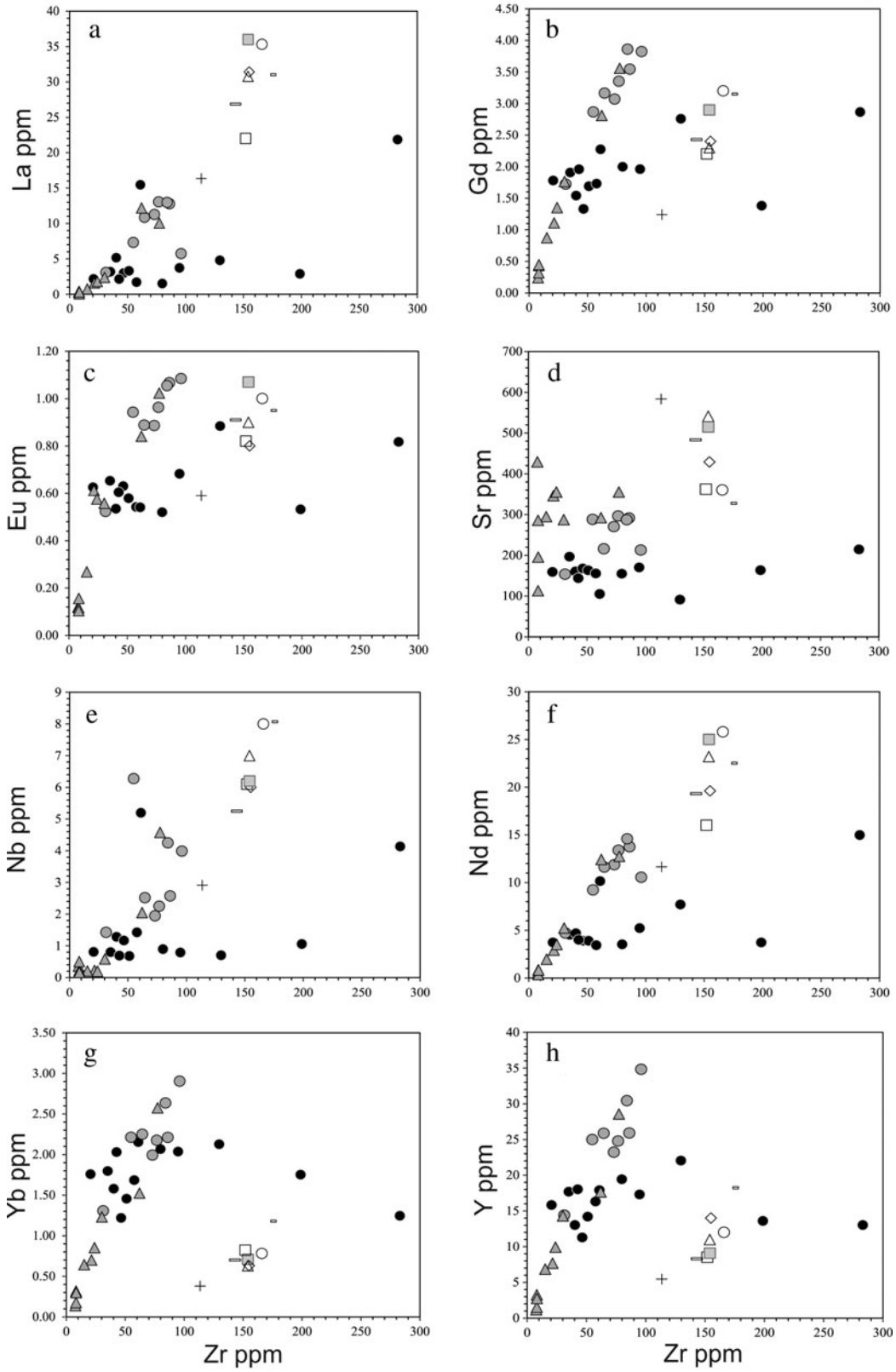

Figure 5. (a–h) Representative trace-element variation plots of the Muslim Bagh Ophiolite plagiogranites. The sheeted dykes and gabbros of the crustal section of the Muslim Bagh Ophiolite (data from Kakar *et al*. 2014) and Archaean TTG average compositions are also plotted; symbols and references as in Figure 3.

https://doi.org/10.1017/S0016756818000250 Published online by Cambridge University Press

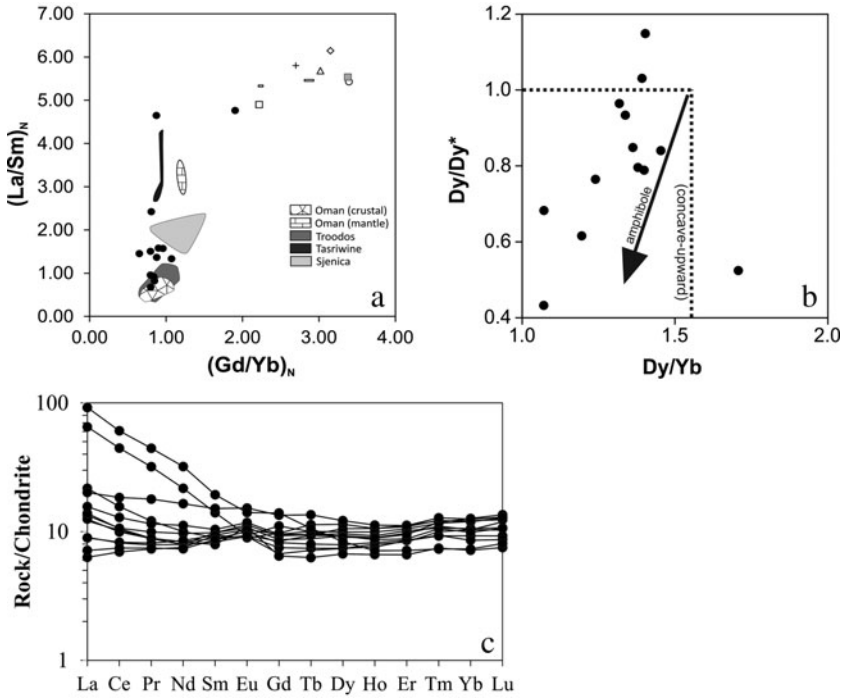

Figure 6. (a) Plot of $(La/Sm)_N$ v. $(Gd/Yb)_N$ highlighting the LREE-enriched nature of the majority of the Muslim Bagh Ophiolite plagiogranites relative to the depleted Oman (Rollinson, 2009) and Troodos Ophiolites (Freund *et al*. 2014). Also plotted are LREE-enriched plagiogranites from the Sjenica (Milovanovic *et al*. 2012) and Tasriwine Ophiolites (Samson *et al*. 2004) and Archaean TTG average compositions (symbols and references as in Fig. 3). (b) Plot of Dy/Dy* v. Dy/Yb showing the majority of the Muslim Bagh Ophiolite plagiogranites to plot in the concave-upwards quadrant (black dotted lines) and follow the amphibole vector (arrow) in figure 4 of Davidson, Turner & Plank (2012). The plot quantifies the degree of concavity, and supports a role for amphibole in the petrogenesis of the plagiogranites either as a residual or crystallizing phase. (c) Chondrite-normalized REE plot of the Muslim Bagh Ophiolite plagiogranites. Normalizing values after Sun & McDonough (1989).

crystallization, partial melting or silicate–liquid immiscibility are variously proposed as petrogenetic models (see Koepke *et al*. 2007 for a review). In the following sections, we discuss the implications the plagiogranite compositions have for each of the possible petrogenetic models.

6.a.1. Fractional crystallization and liquid immiscibility

The layered gabbros and sheeted dykes of the MBO crustal section represent possible cumulates and parental melts, respectively, from which to derive the plagiogranites by crystallization. However, major- and trace-element variation diagrams (Figs 3, 5) show that the plagiogranites do not plot along the same liquid lines of descent as any of the other MBO units. The fact that the plagiogranites define their own distinct field clearly indicates that they are not related to the other units by simple fractional crystallization processes. The lack of intermediate units within the ophiolite sequence also argues against an origin for the plagiogranites by fractional crystallization from a basic parental melt. Additionally, the narrow SiO_2 range of the plagiogranites would suggest that fractional crystallization did not play a primary role in their petrogenesis.

Concave-upwards patterns displayed by the plagiogranites (Fig. 6c) support a role for amphibole during their petrogenesis, as a result of amphiboles preference for MREE over LREE and HREE (e.g. Davidson, Turner & Plank, 2012). However, the concave-upwards pattern on its own does not indicate whether amphibole was crystallizing from a parental magma or acting as a residual phase during the fusion of a mafic protolith.

An origin by silicate–liquid immiscibility (e.g. Dixon & Rutherford, 1979) is also unlikely for the MBO plagiogranites. This is evidenced by the absence of the associated immiscible Fe-rich liquid (as Fe-rich mafic units) from the MBO.

6.a.2. Partial melting

Experimental work of Koepke *et al*. (2004) and France *et al*. (2010) has shown that low TiO_2 contents (<1 wt %) are characteristic of oceanic plagiogranites derived through partial melting of a mafic protolith; this is a consequence of the gabbroic protoliths having initially low TiO_2 contents, typical of cumulate gabbros of the oceanic crust (Koepke *et al*. 2004, 2007). Low TiO_2 contents of the MBO plagiogranites (Fig. 3b) are similar to those in the experimentally derived high-SiO_2 melts of Koepke *et al*. (2004), suggesting they were derived by partial melting of a gabbroic protolith in the crustal sequence of the MBO. In addition, TiO_2 contents of the MBO plagiogranites plot below the boundary line drawn by Koepke *et al*. (2007)

https://doi.org/10.1017/S0016756818000250 Published online by Cambridge University Press

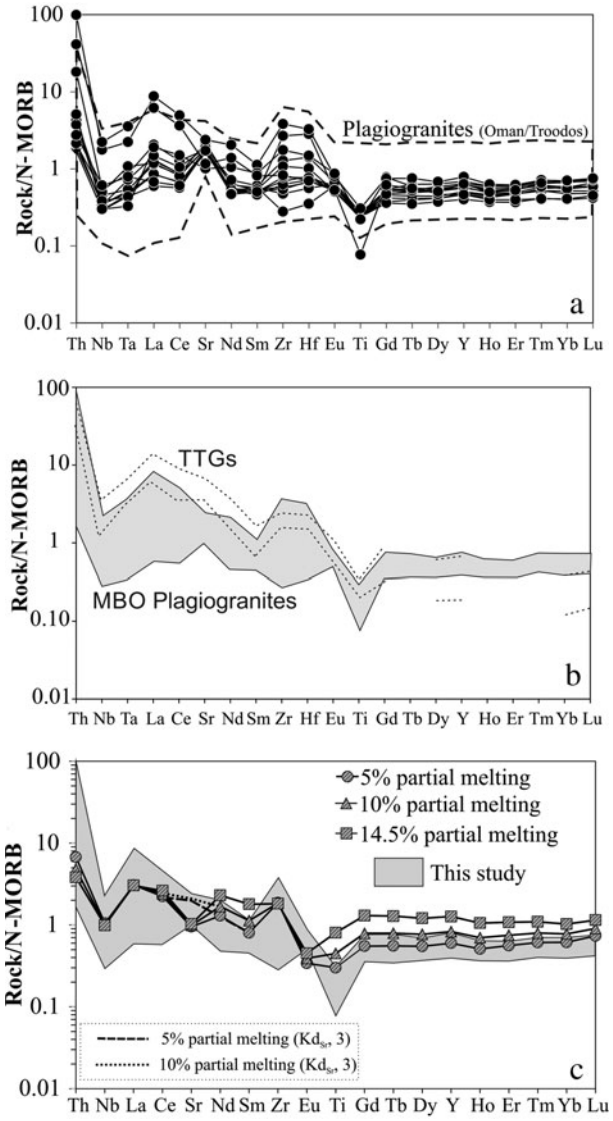

Figure 7. (a) Normal-MORB normalized multi-element plot of the Muslim Bagh Ophiolite plagiogranites. Dashed plagiogranite field represents analyses of plagiogranites from the Troodos (Freund *et al*. 2014) and Oman (Rollinson, 2009) Ophiolites. (b) Normal-MORB normalized multi-element plot comparing the Muslim Bagh Ophiolite plagiogranites with Archaean TTG average compositions (Condie, 2005; Martin *et al*. 2005; Moyen & Martin, 2012). (c) Trace-element modelling of batch melting. The primitive mantle-normalized multi-element plot compares the trace-element composition resulting from trace-element melt modelling of a crustal hornblende gabbro with the composition of the Muslim Bagh Ophiolite plagiogranites. Plagiogranite compositions can be replicated by 5–10 % partial melting of a hornblende gabbro. Dashed black lines represent melts derived by partial melting when using a lower (i.e. 3; Laurent *et al*. 2013) partition coefficient for Sr in plagioclase. Normalizing values after Sun & McDonough (1989).

which separates plagiogranites derived by hydrous partial melting (plot below black dashed line, Fig. 3b) from those plagiogranites derived by crystallization or immiscibility processes (plot above black dashed line).

Additionally, as shown in Figure 3, major-element concentrations of the MBO plagiogranites are similar to Archaean TTG (Condie, 2005; Martin *et al*. 2005; Moyen & Martin, 2012), generally regarded to have been generated through partial melting of a mafic igneous protolith (e.g. Drummond, Defant & Kepezhinskas, 1996; Foley, Tiepolo & Vannucci, 2002; Rapp, Shimizu & Norman, 2003; Martin *et al*. 2005; Moyen & Stevens, 2006; Nutman *et al*. 2009; Hastie *et al*. 2015, 2016). We suggest that the lower K_2O contents displayed by the plagiogranites, compared with Archaean TTG, is the result of the TTG rocks being derived from a more primitive mantle prior to continental crust extraction, and therefore a less-depleted mantle than the present. Trace-element variation plots (Fig 5) do not show as convincing a similarity between the MBO plagiogranites and Archaean TTG as the major-element variation plots (Fig. 3), however. Nevertheless, the MBO plagiogranites have broadly similar trace-element compositions to Archaean TTG (Fig. 7b).

Negative Eu and Sr anomalies (Fig. 6c, 7a) and decreasing Al_2O_3 with increasing SiO_2 (Fig. 3) in some samples could potentially be explained by a small amount of late-stage plagioclase fractional crystallization. However, negative Eu and Sr anomalies can also be the result of plagioclase in the melting residue, while the decrease in Al_2O_3 with SiO_2 can be reproduced through small degrees of partial melting as demonstrated by Beard & Lofgren (1991). In the following section we use trace-element modelling to test a partial melting model for the MBO plagiogranites.

6.b. Modelling of partial melting

To model the partial melting of a mafic protolith, the non-modal batch melting equation of Shaw (1970) was used for the calculations:

$$C_1 = \frac{C_0}{D_0 + F(1-P)} \quad (1)$$

where C_1 is the concentration of a particular trace element in a resultant melt, C_0 is the concentration of an element in the source region prior to partial melting, F is the mass fraction of melt generated, D_0 is the bulk partition coefficient of an element prior to partial melting and P is the partition coefficient of an element weighted by the proportion contributed by each mineral phase to the melt. Hornblende gabbro, C51 (from Kakar *et al*. 2014) was used as the protolith. This sample was collected from the cumulate sequence of the crustal section of the MBO and was chosen as the protolith since the concave-upwards pattern shown by the plagiogranites suggests that amphibole may have been left behind in the melting residue. The partition coefficients used are those for elements in equilibrium with TTG-like silicic melts from Bedard (2006). Mineral modes of the hornblende gabbro are those of Kakar *et al*. (2014) and Siddiqui *et al*. (1996). Melt modes were calculated using 1 kbar experimental runs from Beard & Lofgren (1991) as they provide enough petrological information to carry out the calculation. Melting was stopped at 14.5 %, as this is the point

https://doi.org/10.1017/S0016756818000250 Published online by Cambridge University Press

at which hornblende is exhausted from the protolith. Mineral and melt modes, partition coefficients, hornblende gabbro starting composition and model results can be found in Supplementary Table S3, available at http://journals.cambridge.org/geo.

Figure 7c shows that the incompatible trace-element patterns (including negative Nb and Ti anomalies and positive Th and Zr anomalies) of the plagiogranites can be replicated by 5–10 % partial melting of the hornblende gabbro. Nonetheless, the modelling generates a larger negative Sr anomaly than seen in the MBO plagiogranites. This result is attributed to the use of a high Sr partition coefficient in plagioclase (6.65; Bedard, 2006) and this discrepancy can be removed if a lower partition coefficient is used (i.e. 3, based on the range reported by Laurent *et al*. 2013).

Despite the evidence supporting a partial melting model for the MBO plagiogranites, the reason behind the negative K_2O trend displayed by the plagiogranites when plotted against SiO_2 (Fig. 3) is uncertain. It is however possible that the negative trends displayed by both K_2O and Al_2O_3 are the result of an interplay between fractional crystallization (plagioclase and biotite?) and/or varying degrees of partial melting and source variation.

6.c. Comparison with other Tethyan Ophiolite plagiogranites and implications for the tectonomagmatic setting of the MBO

As we have shown, some geochemical characteristics of the MBO plagiogranites (i.e. LREE enriched and concave-upwards MREE patterns) do not conform to the definition of oceanic plagiogranites as proposed by Coleman & Peterman (1975). The results from this study are similar to previous plagiogranite analyses from the MBO presented by Kakar *et al*. (2014), who also report MBO plagiogranites with LREE-enriched patterns (1–7, $(La/Sm)_N$), as well as negative Nb–Ta–Ti anomalies and low TiO_2 contents ($\leq$0.20 wt %).

The MBO plagiogranites are significantly different from those of other Tethyan Ophiolites in terms of both field and geochemical characteristics. First, LREE contents of Troodos and Oman ophiolite crustal plagiogranites are relatively depleted compared with HREE (Fig. 6a) (Rollinson *et al*. 2009; Freund *et al*. 2014); a more depleted source is therefore required for these plagiogranites relative to the MBO plagiogranites. It is however beyond the scope of this study to investigate further the difference in source enrichment between the MBO plagiogranites and those plagiogranites situated in the Oman and Troodos ophiolites. Secondly, the plagiogranites of the MBO are solely located in the crustal section of the ophiolite, whereas geochemically distinct groups of plagiogranites have been identified in crust and mantle sections of the Troodos and Oman ophiolites (Rollinson, 2009, 2014; Freund *et al*. 2014). Thirdly, the MBO plagiogranites are generally smaller intrusive bodies (on a scale of no more than a few metres) than those found in both the Troodos and Oman ophiolites, where plagiogranites range from several tens of metres to kilometre-sized plutons (Rollinson *et al*. 2009; Freund *et al*. 2014).

The poorly developed sheeted dyke complex (Khan, Kerr & Mahmood, 2007; Kakar *et al*. 2014) of the MBO crustal section is likely the result of the imbalance between spreading rate and magma supply in a supra-subduction zone tectonic setting (Robinson *et al*. 2008). Robinson *et al*. (2008) have proposed that both the fore-arc and back-arc of a supra-subduction zone generally experience lower magma supply rates, due to eruptions at the volcanic arc, and high extensional strain rates. The small size, restricted distribution and lack of geochemical variability (i.e. uniform composition) among the MBO plagiogranites could therefore be a result of this decreased magma supply in the supra-subduction zone where the MBO crystallized. Consequently, the decreased magma supply results in a small degree of partial melting of the plagiogranite source (i.e. crustal hornblende gabbros).

6.d. Implications for Archaean TTG genesis

Most previous and current research into Archaean TTG petrogenesis favours models in which juvenile Archaean continental crust is generated by partial melting of mafic igneous protoliths (e.g. Sen & Dunn, 1994; Wolf & Wyllie, 1994; Foley, Tiepolo & Vannucci, 2002; Rapp, Shimizu & Norman, 2003; Moyen & Stevens, 2006; Laurie & Stevens, 2012; Zhang *et al*. 2013; Ziaja *et al*. 2014; Hastie *et al*. 2016), the setting of which is still controversial; both subduction/flat slab subduction/underthrusting (e.g. Drummond, Defant & Kepezhinskas, 1996; Martin *et al*. 2005; Nutman *et al*. 2009; Hastie *et al*. 2015) and intracrustal (Hamilton, 1998; Hawkesworth, Cawood & Dhuime, 2016) settings have been proposed for the derivation of Archaean TTG of various ages.

Since the original definition of oceanic plagiogranites in the mid-1970s by Coleman & Peterman (1975), oceanic plagiogranites have been shown to differ compositionally from Archaean TTG by being less potassic and having MORB-like LREE and flat HREE patterns. Numerous studies on oceanic plagiogranites from the Oman Ophiolite (Rollinson, 2008, 2009, 2014) have suggested that although the Oman Ophiolite plagiogranites have compositions that are similar to oceanic plagiogranites (as defined by Coleman & Peterman, 1975) and differ compositionally from Archaean TTG, they can be instructive on Archaean TTG genesis. Rollinson (2009) noted that, in addition to the conditions of plagiogranite petrogenesis, a source region enriched in LREE is also required in order to generate the LREE-enriched nature of Archaean TTG. Additionally, Rollinson (2008) has suggested that trondhjemite (plagiogranite) petrogenesis in the Oman Ophiolite acts as a possible analogue for the generation of Earth's first felsic crust during Hadean time. Rollinson (2008) has argued that early (Hadean) felsic crust was of low

https://doi.org/10.1017/S0016756818000250 Published online by Cambridge University Press

volume, and this corresponds to the low volume of plagiogranites we see in recent ophiolite sequences.

The MBO plagiogranites are compositionally different (LREE-enriched and concave-upwards MREE patterns) from the original oceanic plagiogranite definition, but are geochemically similar to Archaean TTG (e.g. Condie, 2005; Martin *et al*. 2005; Moyen & Martin, 2012) (Figs 3, 7b). Consequently, the MBO plagiogranites can be used as a recent (Late Cretaceous) analogue to investigate the formation of some Archaean TTG rocks.

The MBO plagiogranites are found within mafic crust that was formed at a convergent margin, specifically the upper plate above the subduction zone (e.g. Siddiqui *et al*. 1996, 2011; Kakar *et al*. 2014). The similarity in composition between the MBO plagiogranites and Archaean TTG suggests that some of the earliest silicic continental crust may have been derived from melting the overriding plates in primitive subduction-like zones. We acknowledge that there is a contrast in volume between the MBO plagiogranites and Archaean TTG; however, we infer that the genesis of these plagiogranites can be instructive on the generation of some, but not all, Archaean TTG. In addition, the overall greater enrichment in LREE relative to HREE of Archaean TTG compared with the MBO plagiogranites suggests that to source a larger portion of Archaean TTG requires a slightly more enriched source than that of the MBO plagiogranites (e.g. Rollinson, 2009). Again, this could possibly be due to the extraction of continental crust and depletion of the mantle over time.

7. Conclusions

1. Oceanic plagiogranites of the MBO are exclusively located at the base and middle portions of the sheeted dyke complex, where they form small, intrusive dyke-like bodies and lenses.

2. Low TiO_2 contents (<0.4 wt %) in the plagiogranites and a lack of intermediate rocks in the sheeted dyke complex suggest an origin by partial melting of mafic rocks. This is confirmed by batch melt trace-element modelling of a crustal hornblende gabbro from the crustal sequence of the MBO. This modelling shows that the plagiogranites can be replicated by 5–10 % partial melting, possibly with a small degree of late-stage fractional crystallization of plagioclase(?) to account for negative Sr and Eu anomalies and a decrease in Al_2O_3 with SiO_2.

3. The similarity in composition of the MBO plagiogranites to Archaean TTG rocks supports the model that some Archaean TTG could be generated by partial melting of a mafic protolith, possibly in the overriding plate of a subduction-like zone.

Acknowledgements. Iain McDonald is thanked for the major- and trace-element analyses of the samples. We also thank Ahmed Shah, Inayatullah and Akbar for assistance during fieldwork. The Volcanology Igneous Petrology Experimental Research (VIPER) Workshop of the University of Birmingham is thanked for access for petrological study of the samples. Hugh Rollinson is thanked for comments on an earlier draft which substantially improved the manuscript. S. Nasir, S. Köksal and an anonymous reviewer are also thanked for their careful and well-considered reviews which have improved the manuscript. This research received no specific grant from any funding agency, commercial or not-for-profit sectors.

Declaration of interest

None.

Supplementary material

To view supplementary material for this article, please visit https://doi.org/10.1017/S0016756818000250

References

Ahmad, Z. & Abbas, S. G. 1979. The Muslim Bagh Ophiolites. In *Geodynamics of Pakistan* (eds A. Farah & A. DeJong), pp. 243–51. Pakistan: Geological Survey of Pakistan.

Amri, I., Benoit, M. & Ceuleneer, G. 1996. Tectonic setting for the genesis of oceanic plagiogranites: evidence from a paleo-spreading structure in the Oman Ophiolite. *Earth and Planetary Science Letters* **139**, 177–94.

Aranovich, L. Y., Bortnikov, N. S., Serebryakov, N. S. & Sharkov, E. V. 2010. Conditions of the formation of plagiogranite from the Markov Trough, Mid-Atlantic Ridge, 5° 52′-6° 02′ N. *Doklady Earth Sciences* **434**, 1257–62.

Asrarullah, Ahmad, Z. & Abbas, S. G. 1979. Ophiolites in Pakistan: an introduction. In *Geodynamics of Pakistan* (eds A. Farah & A. DeJong), pp. 181–92. Pakistan: Geological Survey of Pakistan.

Barker, F. 1979. Trondhjemite: definition, environment and hypothesis of origin. In *Trondhjemites, Dacites, and Related Rocks* (ed. F. Barker), pp. 1–12. Amsterdam: Elsevier.

Beard, J. S. & Lofgren, G. E. 1991. Dehydration melting and water-saturated melting of basaltic and andesitic greenstones and amphibolites at 1, 3 and 6.9 kb. *Journal of Petrology* **32**, 365–401.

Bedard, J. H. 2006. A catalytic delamination-driven model for coupled genesis of Archean crust and sub-continental lithospheric mantle. *Geochimica et Cosmochimica Acta* **70**, 1188–214.

Coleman, R. G. & Donato, M. M. 1979. Oceanic plagiogranite revisited. In *Trondhjemites, Dacites, and Related Rocks* (ed. F. Barker), pp. 149–68. Amsterdam: Elsevier.

Coleman, R. G. & Peterman, Z. E. 1975. Oceanic plagiogranite. *Journal of Geophysical Research* **80**, 1099–108.

Condie, K. C. 2005. TTGs and adakites: are they both slab melts? *Lithos* **80**, 33–44.

Davidson, J., Turner, S. & Plank, T. 2012. Dy/Dy*: Variations arising from mantle sources and petrogenetic processes. *Journal of Petrology* **54**, 525–37.

Dick, H. J. B., Natland, J. H., Alt, J. C., Bach, W., Bideau, D., Gee, J. S., Haggas, S., Hertogen, J. G. H., Hirth, G., Holm, P. M., Ildefonse, B., Iturrino, G. J., John, B. E., Kelley, D. S., Kikawa, E., Kingdon, A.,

LeRoux, P. J., Maeda, J., Meyer, P. S., Miller, J., Naslund, H. R., Niu, Y. -L., Robinson, P. T., Snow, J., Stephen, R. A., Trimby, P. W., Worm, H. -U. & Yoshinobu, A. 2000. A long in situ section of the lower crust: results of ODP Leg 176 drilling at the Southwest Indian Ridge. *Earth and Planetary Science Letters* **179**, 31–51.

Dixon, S. & Rutherford, M. J. 1979. Plagiogranites as late-stage immiscible liquids in ophiolite and mid-ocean ridge suites an experimental study. *Earth and Planetary Science Letters* **45**, 45–60.

Drummond, M. S., Defant, M. J. & Kepezhinskas, P. K. 1996. Petrogenesis of slab-derived trondhjemite-tonalite-dacite/adakite magmas. *Transactions of the Royal Society of Edinburgh* **87**, 205–15.

Erdmann, M., Fischer, L. A., France, L., Zhang, C., Godard, M. & Koepke, J. 2015. Anatexis at the roof of an oceanic magma chamber at IODP Site 1256 (equatorial Pacific): an experimental study. *Contributions to Mineralogy and Petrology* **169**, 1–28.

Flagler, P. A. & Spray, J. G. 1991. Generation of plagiogranite by amphibolite anatexis in oceanic shear zones. *Geology* **19**, 70–3.

Floyd, P. A. & Winchester, J. A. 1975. Magma type and tectonic setting discrimination using immobile elements. *Earth and Planetary Science Letters* **27**, 211–8.

Foley, S. F., Tiepolo, M. & Vannucci, R. 2002. Growth of early continental crust controlled by melting of amphibolite in subduction zones. *Nature* **417**, 837–40.

France, L., Ildefonse, B. & Koepke, J. 2009. Interactions between magma and hydrothermal system in Oman Ophiolite and in IODP Hole 1256D: fossilization of a dynamic melt lens at fast spreading ridges. *Geochemistry, Geophysics, Geosystems* **10**, 1–30.

France, L., Koepke, J., Ildefonse, B., Cichy, S. B. & Deschamps, F. 2010. Hydrous partial melting in the sheeted dike complex at fast spreading ridges: experimental and natural observations. *Contributions to Mineralogy and Petrology* **160**, 683–704.

Freund, S., Haase, K. M., Keith, M., Beier, C. & Garbe-Schonberg, D. 2014. Constraints on the formation of geochemically variable plagiogranite intrusions in the Troodos Ophiolite, Cyprus. *Contributions to Mineralogy and Petrology* **167**, 1–22.

Gerlach, D. C., Leeman, W. P. & Ave Lallemant, H. G. 1981. Petrology and geochemistry of plagiogranite in the Canyon Mountain Ophiolite, Oregon. *Contributions to Mineralogy and Petrology* **77**, 82–92.

Gillis, K. M. & Coogan, L. A. 2002. Anatectic migmatites from the roof of an ocean ridge magma chamber. *Journal of Petrology* **43**, 2075–95.

Gnos, E., Immenhauser, A. & Peters, T. 1997. Late Cretaceous/early Tertiary convergence between the Indian and Arabian plates recorded in ophiolites and related sediments. *Tectonophysics* **271**, 1–19.

Grimes, C. B., Ushikubo, T., John, B. E. & Valley, J. W. 2011. Uniformly mantle-like Delta18O in zircons from oceanic plagiogranites and gabbros. *Contributions to Mineralogy and Petrology* **161**, 13–33.

Hamilton, W. B. 1998. Archean magmatism and deformation were not products of plate tectonics. *Precambrian Research* **91**, 143–79.

Hastie, A. R., Fitton, J. G., Bromiley, G. D., Butler, I. B. & Odling, N. W. A. 2016. The origin of Earth's first continents and the onset of plate tectonics. *Geology* **44**, 855–8.

Hastie, A. R., Fitton, J. G., Mitchell, S. F., Neill, I. M., Nowell, G. & Millar, I. L. 2015. Can fractional crystallization, mixing and assimilation processes be responsible for Jamaican-type adakites? Implications for generating EoArchean continental crust. *Journal of Petrology* **56**, 1251–84.

Hastie, A. R., Kerr, A. C., Mitchell, S. F. & Millar, I. L. 2009. Geochemistry and tectonomagmatic significance of lower Cretaceous island arc lavas from the Devils Racecourse Formation, eastern Jamaica. In *The Origin and Evolution of the Caribbean Plate* (eds K. H. James, M. A. Lorente & J. L. Pindell), pp. 339–60. Geological Society of London, Special Publication no. 328.

Hastie, A. R., Kerr, A. C., Pearce, J. A. & Mitchell, S. F. 2007. Classification of altered volcanic island arc rocks using immobile trace elements: development of the Th-Co discrimination diagram. *Journal of Petrology* **48**, 2341–57.

Hawkesworth, C. J., Cawood, P. A. & Dhuime, B. 2016. Tectonics and crustal evolution. *GSA Today* **26**, 4–11.

Jafri, S. H., Charan, S. N. & Govil, P. K. 1995. Plagiogranite from the Andaman Ophiolite Belt, Bay of Bengal, India. *Journal of the Geological Society, London* **152**, 681–7.

Kakar, M. I., Collins, A. S., Mahmood, K., Foden, J. D. & Khan, M. 2012. U-Pb zircon crystallization age of the Muslim Bagh Ophiolite: Enigmatic remains of an extensive pre-Himalayan arc. *Geology* **40**, 1099–102.

Kakar, M. I., Kerr, A. C., Mahmood, K., Collins, A. S., Khan, M. & McDonald, I. 2014. Supra-subduction zone tectonic setting of the Muslim Bagh Ophiolite, northwestern Pakistan: Insights from geochemistry and petrology. *Lithos* **202–203**, 190–206.

Kasi, A. K., Kassi, A. M., Umar, M., Manan, R. A. & Kakar, M. I. 2012. Revised lithostratigraphy of the Pishin Belt, northwestern Pakistan. *Journal of Himalayan Earth Sciences* **45**, 53–65.

Kaur, G. & Mehta, P. K. 2005. The Gothara plagiogranite: evidence for oceanic magmatism in a non-ophiolitic association, North Khetri Copper Belt, Rajasthan, India? *Journal of Asian Earth Sciences* **25**, 805–19.

Kerrich, R. & Polat, A. 2006. Archean greenstone-tonalite duality: Thermochemical mantle convection models or plate tectonics in the early Earth global dynamics? *Tectonophysics* **415**, 141–65.

Khan, M., Kerr, A. C. & Mahmood, K. 2007. Formation and tectonic evolution of the Cretaceous-Jurassic Muslim Bagh ophiolitic complex, Pakistan: implications for the composite tectonic setting of ophiolites. *Journal of Asian Earth Sciences* **31**, 112–27.

Khan, S. D., Mahmood, K. & Casey, J. F. 2007. Mapping of Muslim Bagh ophiolite complex (Pakistan) using new remote sensing, and field data. *Journal of Asian Earth Sciences* **30**, 333–43.

Khan, S. D., Walker, D. J., Hall, S. A., Burke, K. C., Shah, M. T. & Stockli, L. 2009. Did the Kohistan-Ladakh island arc collide first with India? *Bulletin of the Geological Society of America* **121**, 366–84.

Koepke, J., Berndt, J., Feig, S. T. & Holtz, F. 2007. The formation of SiO2-rich melts within the deep oceanic crust by hydrous partial melting of gabbros. *Contributions to Mineralogy and Petrology* **153**, 67–84.

Koepke, J., Feig, S. T., Snow, J. & Freise, M. 2004. Petrogenesis of oceanic plagiogranites by partial melting of gabbros: an experimental study. *Contributions to Mineralogy and Petrology* **146**, 414–32.

Kusky, T. M., Windley, B. F., Safonova, I., Wakita, K., Wakabayashi, J., Polat, A. & Santosh, M. 2013. Recognition of ocean plate stratigraphy in accretionary orogens through Earth history: a record of 3.8 billion years of sea floor spreading, subduction, and accretion. *Gondwana Research* **24**, 501–47.

Laurent, O., Doucelance, R., Martin, H. & Moyen, J. F. 2013. Differentiation of the late-Archean sanukitoid series and some implications for crustal growth: Insights from geochemical modelling on the Bulai pluton, Central Limpopo Belt, South Africa. *Precambrian Research* **227**, 186–203.

Laurie, A. & Stevens, G. 2012. Water-present eclogite melting to produce Earth's early felsic crust. *Chemical Geology* **314–317**, 83–95.

Le Maitre, R. W., Streckeisen, A., Zanettin, B., Le Bas, M. J., Bonin, B. & Bateman, P. (eds) 2002. *Igneous Rocks : A Classification and Glossary of Terms*. Cambridge: Cambridge University Press.

Mahmood, K., Boudier, F., Gnos, E., Monie, P. & Nicolas, A. 1995. 40Ar/39Ar dating of the emplacement of the Muslim Bagh Ophiolite, Pakistan. *Tectonophysics* **250**, 169–81.

Martin, H., Smithies, R. H., Rapp, R., Moyen, J. F. & Champion, D. 2005. An overview of adakite, tonalite-trondhjemite-granodiorite (TTG), and sanukitoid: Relationships and some implications for crustal evolution. *Lithos* **79**, 1–24.

McDonald, I. & Viljoen, K. S. 2006. Platinum-group element geochemistry of mantle eclogites: a reconnaissance study of xenoliths from the Orapa kimberlite, Botswana. *Applied Earth Science* **115**, 81–93.

Mengal, J. M., Kimura, K., Siddiqui, R. H., Kojima, S., Naka, T., Bakht, M. S. & Kamada, K. 1994. The lithology and structure of a Mesozoic sedimentary-igneous assemblage beneath the Muslim Bagh Ophiolite, northern Balochistan, Pakistan. *Bulletin of the Geological Survey of Japan* **2**, 51–61.

Milovanovic, D., Sreckovic-Batocanin, D., Savic, M. & Popovic, D. 2012. Petrology of plagiogranite from Sjenica, Dinaridic Ophiolite Belt (southwestern Serbia). *Geologica Carpathica* **63**, 97–106.

Moyen, J. F. & Martin, H. 2012. Forty years of TTG research. *Lithos* **148**, 312–36.

Moyen, J. F. & Stevens, G. 2006. Experimental constraints on TTG petrogenesis: implications for Archean geodynamics. In *Archean Geodynamics and Environments* (eds K. Benn, J. -C. Mareschal & K. C. Condie), pp. 149–75. American Geophysical Union, Washington D.C., Geophysical Monograph no. 164.

Nakamura, K., Morishita, T., Chang, Q., Neo, N. & Kumagai, H. 2007. Discovery of lanthanide tetrad effect in an oceanic plagiogranite from an ocean core complex at the Central Indian Ridge 25S. *Geochemical Journal* **41**, 135–40.

Nutman, A. P., Bennett, V. C., Friend, C. R. L., Jenner, F., Wan, Y. & Liu, D. 2009. EoArchean crustal growth in west Greenland (Itsaq Gneiss Complex) and in north-eastern China (Anshan area): review and synthesis. In *Earth Accretionary Systems in Space and Time* (eds P. A. Cawood & A. Kröner), pp. 127–54. Geological Society of London, Special Publication no. 318.

Pearce, J. A. & Peate, D. W. 1995. Tectonic implications of the composition of volcanic arc magmas. *Annual Review of Earth and Planetary Sciences* **23**, 251–85.

Qayyum, M., Niem, A. R. & Lawrence, R. D. 1996. Newly discovered Paleogene deltaic sequence in Katawaz Basin, Pakistan, and its tectonic implications. *Geology* **24**, 835–8.

Rao, D. R., Rai, H. & Kumar, J. S. 2004. Origin of oceanic plagiogranite in the Nidar ophiolitic sequence of eastern Ladakh, India. *Current Science* **87**, 999–1005.

Rapp, R. P., Shimizu, N. & Norman, M. D. 2003. Growth of early continental crust by partial melting of eclogite. *Nature* **425**, 605–9.

Robinson, P. T., Malpas, J., Dilek, Y. & Zhou, M. 2008. The significance of sheeted dike complexes in ophiolites. *GSA Today* **18**, 4–10.

Rollinson, H. 2008. Ophiolitic trondhjemites: a possible analogue for Hadean felsic "crust." *Terra Nova* **20**, 364–69.

Rollinson, H. 2009. New models for the genesis of plagiogranites in the Oman Ophiolite. *Lithos* **112**, 603–14.

Rollinson, H. 2014. Plagiogranites from the mantle section of the Oman Ophiolite: models for early crustal evolution. In *Tectonic Evolution of the Oman Mountains* (eds H. R. Rollinson, M. P. Searle, I. A. Abbasi, A. I. Al-Lazki & M. H. Al Kindi), pp. 247–61. Geological Society of London, Special Publication no. 392.

Samson, S. D., Inglis, J. D., D'Lemos, R. S., Admou, H., Blichert-Toft, J. & Hefferan, K. 2004. Geochronological, geochemical, and Nd-Hf isotopic constraints on the origin of Neoproterozoic plagiogranites in the Tasriwine Ophiolite, Anti-Atlas orogen, Morocco. *Precambrian Research* **135**, 133–47.

Sawada, Y., Nagao, K., Siddiqui, R. H. & Khan, S. R. 1995. K-Ar ages of the Mesozoic igneous and metamorphic rocks from the Muslim Bagh area, Pakistan. *Proceedings of Geoscience Colloquium* **12**, 73–90.

Sen, C. & Dunn, T. 1994. Dehydration melting of a basaltic composition amphibolite at 1.5 and 2.0 GPa: implications for the origin of adakites. *Contributions to Mineralogy and Petrology* **117**, 394–409.

Shaw, D. M. 1970. Trace element fractionation during anatexis. *Geochimica et Cosmochimica Acta* **34**, 237–43.

Siddiqui, R. H., Aziz, A., Mengal, J. M., Hoshino, K. & Sawada, Y. 1996. Geology, petrochemistry and tectonic evolution of the Muslim Bagh Ophiolite Complex, Pakistan. *Proceedings of Geoscience Colloquium* **16**, 11–46.

Siddiqui, R. H., Mengal, J. M., Hoshino, K., Sawada, Y. & Brohi, I. A. 2011. Back-arc basin signatures represented by the sheeted dykes from the Muslim Bagh Ophiolite Complex, Balochistan, Pakistan. *Sindh University Research Journal* **43**, 51–62.

Sun, S.-S. & McDonough, W. F. 1989. Chemical and isotopic systematics of oceanic basalts: implications for mantle composition and processes. In *Magmatism in the Ocean Basins* (eds A. D. Saunders & M. J. Norry), pp. 313–45. Geological Society of London, Special Publication no. 42.

Tilton, G. R., Hopson, C. A. & Wright, J. E. 1981. Uranium-lead isotopic ages of the Samail Ophiolite, Oman, with applications to Tethyan Ocean ridge tectonics. *Journal of Geophysical Research: Solid Earth* **86**, 2763–75.

Twining, K. 1996. Origin of plagiogranite in the Troodos ophiolite, Cyprus. In *Proceedings of the 9th Keck Symposium in Geology*, pp. 245–8. Williamstown, MA, 1 April 1996.

Wolf, M. B. & Wyllie, P. J. 1994. Dehydration-melting of amphibolite at 10 kbar: the effects of temperature and time. *Contributions to Mineralogy and Petrology* **115**, 369–83.

Yaliniz, M. K., Floyd, P. A. & Goncuoglu, M. C. 2000. Petrology and geotectonic significance of plagiogranite from the Sarikaraman Ophiolite (Central Anatolia, Turkey). *Ofioliti* **1**, 31–7.

Zhang, C., Holtz, F., Koepke, J., Wolff, P. E., Ma, C. & Bédard, J. H. 2013. Constraints from experimental melting of amphibolite on the depth of formation of garnet-rich restites, and implications for models of Early Archean crustal growth. *Precambrian Research* **231**, 206–17.

Ziaja, K., Foley, S. F., White, R. W. & Buhre, S. 2014. Metamorphism and melting of picritic crust in the early Earth. *Lithos* **189**, 173–84.

https://doi.org/10.1017/S0016756818000250 Published online by Cambridge University Press